Synergistic Effects of Crizotinib and Temozolomide in Experimental FIG-ROS1 Fusion-Positive Glioblastoma

Arabinda Das[1], Ron Ron Cheng[1], Megan L.T. Hilbert[1], Yaenette N. Dixon-Moh[1], Michele Decandio[1], William Alex Vandergrift III[1], Naren L. Banik[1,2], Scott M. Lindhorst[1], David Cachia[1], Abhay K. Varma[1], Sunil J. Patel[1] and Pierre Giglio[1,3]

[1]Department of Neurosurgery, Medical University of South Carolina, Charleston, SC, USA. [2]Ralph H. Johnson VA Medical Center, Charleston, SC, USA. [3]Department of Neurological Surgery, The Ohio State University Wexner Medical Center, Columbus, OH, USA.

ABSTRACT: Glioblastoma (GB) is the most common malignant brain tumor. Drug resistance frequently develops in these tumors during chemotherapy. Therefore, predicting drug response in these patients remains a major challenge in the clinic. Thus, to improve the clinical outcome, more effective and tolerable combination treatment strategies are needed. Robust experimental evidence has shown that the main reason for failure of treatments is signal redundancy due to coactivation of several functionally linked receptor tyrosine kinases (RTKs), including anaplastic lymphoma kinase (ALK), c-Met (hepatocyte growth factor receptor), and oncogenic c-ros oncogene1 (ROS1: RTK class orphan) fusion kinase FIG (fused in GB)-ROS1. As such, these could be attractive targets for GB therapy. The study subjects consisted of 19 patients who underwent neurosurgical resection of GB tissues. Our in vitro and ex vivo models promisingly demonstrated that treatments with crizotinib (PF-02341066: dual ALK/c-Met inhibitor) and temozolomide in combination induced synergistic antitumor activity on FIG-ROS1-positive GB cells. Our results also showed that ex vivo FIG-ROS1+ slices (obtained from GB patients) when cultured were able to preserve tissue architecture, cell viability, and global gene-expression profiles for up to 14 days. Both in vitro and ex vivo studies indicated that combination blockade of FIG, p-ROS1, p-ALK, and p-Met augmented apoptosis, which mechanistically involves activation of Bim and inhibition of survivin, p-Akt, and Mcl-1 expression. However, it is important to note that we did not see any significant synergistic effect of crizotinib and temozolomide on FIG-ROS1-negative GB cells. Thus, these ex vivo culture results will have a significant impact on patient selection for clinical trials and in predicting response to crizotinib and temozolomide therapy. Further studies in different animal models of FIG-ROS1-positive GB cells are warranted to determine useful therapies for the management of human GBs.

KEY WORDS: ALK, crizotinib, FIG, glioblastoma, c-Met inhibitor, ROS1, temozolomide

CITATION: Das et al. Synergistic Effects of Crizotinib and Temozolomide in Experimental FIG-ROS1 Fusion-Positive Glioblastoma. *Cancer Growth and Metastasis* 2015:8 51–60 doi:10.4137/CGM.S32801.

TYPE: Original Research

RECEIVED: September 14, 2015. **RESUBMITTED:** October 18, 2015. **ACCEPTED FOR PUBLICATION:** October 20, 2015.

ACADEMIC EDITOR: Marc D. Basson, Editor in Chief

PEER REVIEW: Ten peer reviewers contributed to the peer review report. Reviewers' reports totaled 3389 words, excluding any confidential comments to the academic editor.

FUNDING: This study was supported by Pfizer, Inc., Brain Tumor Research at the MUSC Foundation, and the Department of Neurosurgery (MUSC). The authors confirm that the funder had no influence over the study design, content of the article, or selection of this journal.

COMPETING INTERESTS: Pfizer Inc. supplied crizotinib for this study. The results of this research and any intellectual property arising from this research are subject to existing rights and obligations to a third party, Pfizer Inc.

CORRESPONDENCE: dasa@musc.edu

Paper subject to independent expert blind peer review. All editorial decisions made by independent academic editor. Upon submission manuscript was subject to anti-plagiarism scanning. Prior to publication all authors have given signed confirmation of agreement to article publication and compliance with all applicable ethical and legal requirements, including the accuracy of author and contributor information, disclosure of competing interests and funding sources, compliance with ethical requirements relating to human and animal study participants, and compliance with any copyright requirements of third parties. This journal is a member of the Committee on Publication Ethics (COPE). Provenance: the authors were invited to submit this paper.

Published by Libertas Academica. Learn more about this journal.

Introduction

Glioblastoma (GB) is classified by the World Health Organization as a Grade IV tumor and represents 15%–20% of all primary intracranial tumors.[1–4] It is the most aggressive and malignant of astrocytic tumors, with histopathological features, including cellular pleomorphism, rapid mitotic activity, microvascular proliferation, and necrosis. Approximately 28,000 new cases of malignant gliomas are diagnosed in the US and European Union each year (Source: US National Cancer Registry).[2–4] Currently, combination therapy is an integral component of the multimodal treatment of GB patients. However, despite improvements in drug delivery and novel chemotherapy, the prognosis of patients with GB remains poor. Of those treated with multimodal treatment, there is only a 3.4% survival after five years (Central Brain Tumor Registry).[1–4] It is therefore essential to develop new molecular target-based therapeutic strategies. This approach may prove to be an effective strategy in genetically defined subsets of patients with GB. Treatment of these relatively small subpopulations of GB patients harboring genetic abnormalities translates into a large number of overall patients treated because of the high prevalence of the disease. Because GB is an infiltrative disease that is often resistant to treatment, it is believed that the development of new combinational therapies, together with an increase in the selectivity of the treatments based on a detailed molecular characterization of these tumors, may contribute to enhance the survival of patients suffering from GB. The favorable safety profile of the current standard therapy drug, temozolomide, allows it to be coadministered with various agents.[1–3]

According to the current literature, mutations in the anaplastic lymphoma kinase (ALK) gene and expression levels of the proto-oncogene c-Met correlate with glioma malignancy, with their overexpression linked to shorter survival time and

poorer treatment outcomes.[5–7] Crizotinib, also known as Xalkori, has recently been shown to have superior efficacy on ALK/c-Met-positive tumors in the treatment of advanced cancer patients, which led to its approval by the US Food and Drug Administration (FDA) in 2011 as the first-in-class compound.[8–13] ROS1 is one of the two orphan receptor tyrosine kinases (RTKs), which shares only 49% amino acid sequence homology with ALK in the kinase domains.[14–16] Recently, ROS1 fusions were identified as potential driver mutations in GB.[14–17] Fused in GB (FIG) has also been identified as a potential driver mutation; FIG-derived exons and nine ROS-derived exons represent the first example of an RTK fusion protein that does not arise as a result of a translocation or inversion but rather from a relatively small intrachromosomal homozygous deletion of 240 kb on 6q21.[17] This fusion product is targeted to the Golgi apparatus where it is thought to exert its oncogenic signaling. With the recent US FDA approval of crizotinib, much attention has turned to FIG-ROS1-positive tumors.[18–22] Therefore, it is postulated that patients without ALK rearrangement, but amplification of c-Met or activation of other specific crizotinib targets (ROS1: an oncogenic kinase), may also benefit from crizotinib therapy. Interestingly, published interim analysis results showed no direct impact on overall survival as compared to chemotherapy; though there were high numbers of chemotherapy crossovers to crizotinib, a direct comparison was difficult. In spite of the clinical success with crizotinib, a major obstacle recognized early on was the acquired resistance to treatment.[21]

Here, we sought to explore the efficacy of temozolomide and crizotinib in ALK/c-Met (ALK and c-Met pathway) and FIG-ROS1 fusion-positive GB cells within in vitro standard cell culture systems and ex vivo tissue slices. The special advantage of this ex vivo slice culture approach is the ability to maintain organ and cellular architecture, while also preserving the integrity of the tumor–stroma interaction. No study to date has systematically evaluated the efficacy of ex vivo organotypic culture in GB using slice technology, much less on a heterogeneous pool of tumor samples and compared the effects of crizotinib on ALK/c-Met signaling pathways. Moreover, the exact effects of crizotinib on the downstream signaling pathways that regulate the proliferation or survival of FIG-ROS1-positive GB cells remain to be established, and the combination effects of crizotinib with temozolomide has not been addressed. Given the therapeutic potential of the crizotinib, we hypothesized that combining this agent with temozolomide would result in increased tumor inhibition compared with either agent alone. We used the FIG-ROS1-positive human GB cells in in vitro and ex vivo models to examine how crizotinib affects ALK-Met signaling and its potential as a novel temozolomide-sensitizing agent in GB.

Methods

Ethical considerations. This research was approved by the Institutional Review Board for Human Research, Office of Research Integrity, Medical University of South Carolina (MUSC). Subjects gave their written, informed consent to participate, and the research was conducted in accordance with the principles of the Declaration of Helsinki.

Acquisition of human GB samples. GB patient samples were collected surgically from patients diagnosed with GB according to the Response Assessment in Neuro-Oncology Criteria. Patients were evaluated based on magnetic resonance imaging (MRI), as well as clinical and pathological examination. All the patients were considered to have GB, and after careful review of the clinical information by the multidisciplinary, comprehensive neurosurgery team at the Medical University of South Carolina (MUSC), the tissue was collected and handled according to MUSC procedures with the approval of the Institutional Review Board at the University. The patients who received neoadjuvant chemotherapy and/or radiotherapy before surgery were excluded from the study. The MRI examinations of 19 patients (12 males and 7 females) with GB (confirmed by histopathological examination by a pathologist) were analyzed. MRI examinations were performed preoperatively, within 24 hours postoperatively, and 30 ± 6 days (range 24–36) after surgery (before the beginning of adjuvant chemoradiation).

Tissue slice preparation. Fresh human GB specimens, in addition to those required for neuropathological diagnostic procedures, were obtained after surgical resection or biopsy at the MUSC in Charleston. An overview of the samples used in this study is given in Table 1. During the operative procedure, the surgeon removed specimens from the central portion of the tumor under direct visualization or via biopsy. The majority of each tumor sample was then sliced. The tissue was transported to the laboratory in the minimal essential medium (MEM; Invitrogen). The standard Stoppini Slice Culture Technique was used for these studies.[23] Slice cultures were prepared using a tissue chopper (McIlwain) at a thickness of 250 µm under sterile conditions. Before preparation, a standard razor blade was wiped with ethanol to remove any oil and then sterilized by autoclaving. Additionally, a normal glass pipette and a pipette with the fine tip broken off were autoclaved. If needed, biopsy specimens were cut into appropriately sized pieces first to obtain evenly shaped slices of 5 × 5 mm. When the tissue chopper was used, the tissue was put on a stack of sterile filter membranes, cut, and then transferred carefully into ice-cold MEM by forceps. In most of the preparations, the slices stuck together after cutting, so they were separated under a stereomicroscope with two scalpels without traumatizing the tissue. The slices were then transferred by the glass pipette with a wide opening onto membrane culture inserts (Millipore) in 6-well plates at a maximum of three slices per insert depending on the size. The cultivation medium consisted of MEM (Gibco), 25% Hank's Balanced Salt Solution (with Ca and Mg; Gibco), 20% Horse serum (Gibco), 2 mM L-glutamine (Braun), 0.5% glucose, and 1% penicillin/streptomycin (Sigma). The slices were cultivated on a liquid/air interface in a humidified incubator at 37°C and 5% CO_2, and the medium was changed three times a week. These slices were

Table 1. Background of collected GB patient samples used for slice culture experiments in this study.

PATIENT (PT)	AGE	SEX	TUMOR LOCATION	DIAGNOSIS	EXTENT OF RESECTION	INITIAL KPS	INITIAL THERAPY	THERAPY FOR FIRST PROGRESSION	THERAPIES FOR SUB-SEQUENT PROGRESSION	POST-TREATMENT KPS*	PFS (DAYS)	SURVIVAL (DAYS)
Pt 1	69	F	Right temporal parietal	GB	GTR	90	RTOG-0837: Radiation Temozolomide Cediranib vs. placebo	Bevacizumab	NA	0	157	520
Pt 2†	61	M	Right temporal parietal	GB	Partial	80	Radiation Temozolomide	NA	NA	80	NA	NA
Pt 3	54	F	Right frontal	GB with oligodendrogial component	Partial	90	Radiation Temozolomide	Bevacizumab	Bevacizumab Carboplatin GK SRS	0	140	912
Pt 4	62	M	Right frontal	GB	Partial	90	Radiation Temozolomide DCVax-L trial	CC-122 PO trial Re-resection	NA	0	346	432
Pt 5	43	M	Left temporal	GB with sarcomatoid features	Partial	80	Radiation Temozolomide	Operative debulking Temozolomide	Bevacizumab, Temozolomide Vorinostat Cis-retinoic acid Novocure tumor treatment field therapy Cyclophosphamide	0	87	324
Pt 6	64	M	Left parietal	GB with ependymal features	Partial	80	Radiation Temozolomide	Bevacizumab	Bevacizumab Carboplatin GK SRS CCNU	0	402	858
Pt 7	73	M	Left frontal	GB	Partial	60	None	NA	NA	0	NA	37
Pt 8	58	F	Bifrontal traversing corpus callosum	GB	Partial	80	Radiation Temozolomide	Bevacizumab	NA	0	61	405
Pt 9	72	M	Bifrontal traversing corpus callosum	GB	Partial	100	Radiation Temozolomide	Palliative care	NA	0	162	217
Pt 10	36	M	Left temporal	GB with oligodendrogial component	GTR	100	Radiation Temozolomide	Bevacizumab Metronomic temozolomide	NA	90	458	NA
Pt 11	54	F	Left frontal	GB	Biopsy	90	Radiation Temozolomide Trans-sodium crocetinate trial	Bevacizumab Temozolomide Radiation	NA	0	53	78
Pt 12	60	F	Two right frontal lesions	GB with oligodendrogial component	Partial	90	Radiation Temozolomide	Bevacizumab	Bevacizumab Carboplatin	80	99	NA
Pt 13	59	M	Left temporal	GB	Partial	90	Radiation Temozolomide Everolimus	NA	NA	0	NA	150

(*Continued*)

Table 1. (*Continued*)

PATIENT (PT)	AGE	SEX	TUMOR LOCATION	DIAGNOSIS	EXTENT OF RESECTION	INITIAL KPS	INITIAL THERAPY	THERAPY FOR FIRST PROGRESSION	THERAPIES FOR SUB-SEQUENT PROGRESSION	POST-TREATMENT KPS*	PFS (DAYS)	SURVIVAL (DAYS)
Pt 14	62	F	Right frontal	GB	Partial	90	Radiation Temozolomide	Bevacizumab Chemoradiation	NA	90	57	NA
Pt 15	73	M	Left parietal	GB	Partial	70	Radiation Temozolomide	Bevacizumab	Bevacizumab	60	168	NA
Pt 16	81	F	Right temporal	GB	GTR	90	Radiation Temozolomide Bevacizumab	NA	NA	0	NA	489
Pt 17	66	M	Left basal ganglia	GB	Biopsy	80	Palliative care	NA	NA	0	NA	71
Pt 18	58	M	Bifrontal traversing corpus callosum	GB	Partial	90	Radiation Temozolomide	Bevacizumab GK SRS Cis-retinoic acid	Retinoid therapy Bevacizumab	0	91	349
Pt 19	73	M	Right temporal	GB	Partial	90	Radiation Temozolomide	NA	NA	0	NA	149

Notes: [1]KPS at last documented follow-up. KPS 0 indicates death during follow-up period. [2]Patient was unable to obtain postop MRI with gadolinium due to end-stage renal disease and was also lost to follow-up.
Abbreviations: GB, glioblastoma multiforme; GTR, gross total resection; KPS, Karnofsky Performance Status; GK SRS, Gamma Knife stereotactic radiosurgery; PFS, progression-free survival.

well maintained, with histological preservation of the main features of the original tumor for at least 14 days.

Cell and slice culture treatment studies. Human GB U118MG (FIG-ROS1-positive) and U87MG (FIG-ROS1-negative) cells were purchased from American Type Culture Collection and were maintained in 75 cm^3 flasks under a humidified atmosphere of 5% CO_2 at 37°C in Dulbecco's Modified Eagle Medium (DMEM) 1× medium and Roswell Park Memorial Institute (RPMI) 1640 1× medium (Sigma), respectively, and both were supplemented with 5% fetal bovine serum. GB cells and tissue slices were incubated with crizotonib (200 nM [cells]/2 μM [slice cultures]) and temozolomide (5 μM [cells]/50 μM [slice cultures]) for 48 hours for induction of apoptosis. These concentrations of crizotonib and temozolomide were determined to inhibit 25% (IC_{25}) of proliferation during in vitro studies and were then used to test the effectiveness of the combination of crizotinib and temozolomide in these cell lines. In the case of the slice culture, we used ten times more drug (concentration-wise) as compared to cell culture. After treatment, the slices were snap frozen for Western blots and some slices were formalin fixed and paraffin embedded for immunohistochemistry (IHC) evaluation. All the cells and tissue slices were used for the evaluation of mechanisms of apoptosis, gene expression, and phospho-activation of selected targets in the ALK/c-Met pathway.[24–27]

Cells and tissue-viability analysis. A total of 5×10^4 U118 and U87MG cells per well were seeded into a 6-well plate overnight, and the tissue slices were grown in culture inserts (Millipore) in 6-well plates. Dose–response studies were conducted to determine the suitable concentration of the drugs used in the cell culture and tissue slice experiments. Cells and tissue slices were treated with crizotonib (200 nM [cells]/2 μM [slice cultures]) and temozolomide (5 μM [cells]/50 μM [slice cultures]) for 48 hours. Next, they were incubated with 5 mg/mL of 4,5-dimethylthiazol-2-yl-2,5-diphenyltetrazoliumbromide (MTT) at 37°C for four hours. The culture supernatant was then removed and dimethyl sulfoxide (DMSO) (for cells) or 0.1M HCl-isopropyl alcohol (for tissue slices) was added (500 μL/well). Cells were incubated in a shaker at 37°C for 25 minutes until the crystals were completely dissolved. A total of 96-well plates were used to measure the absorbance using the EMax Precision Microplate reader at 570 nm with the reference wavelength set at 620 nm using SoftMax Pro software (Molecular Devices). Optical density was compared by setting the control at 100% and the results were analyzed using Microsoft Office Excel ©. This experiment was performed in triplicate and repeated three times. Calculation of cell viability was described previously.[24]

Analysis of DNA fragmentation. Genomic DNA fragmentation was analyzed by agarose gel electrophoresis of genomic DNA isolated from GB tissues, as reported previously.[25]

Determination of ROS production. The fluorescent probe 2′,7′-dichlorofluorescin diacetate (DCF-DA) was used for the assessment of intracellular ROS production. This is a reliable method for the measurement of intracellular ROS such as hydrogen peroxide (H_2O_2), hydroxyl radical, and hydroperoxides, as reported previously.[26] Spectramax Gemini XPS (Molecular Devices) was used to evaluate the change in fluorescence. The increase in fluorescence intensity was used to assess the generation of net intracellular ROS.

Apoptosis determined by flow cytometry. The apoptotic response after crizotinib and temozolomide treatment was measured by flow cytometry using the Annexin V-FITC Apoptosis Detection Kit. The samples were analyzed by a CyAn ADP desktop analyzer (MUSC). For each sample, 10,000 cells were analyzed. The number of apoptotic cells was calculated using the Cell Quest software.

Ki-67/GFAP immunofluorescent staining. Ki-67/glial fibrillary acidic protein (GFAP) immunofluorescent staining was performed using our laboratory standard protocol. We used primary rabbit monoclonal anti-human Ki-67 (AbCam) and rabbit polyclonal anti-GFAP (Cell Signaling) for IHC. At the same time, we mounted the slides with VECTASHIELD® containing 4',6-diamidino-2-phenylindole (DAPI) nuclear stain. A minimum of three 200× magnification images were captured for each section using a Zeiss fluorescent microscope (Carl Zeiss, Inc.) from the Storm Eye Institute, MUSC. The images were compiled and processed using Adobe Photoshop Elements.

Western blot analysis. Western blotting was performed as described previously.[24–26] Monoclonal antibody (mAb) against glyceraldehyde-3-phosphate dehydrogenase (GAPDH) antibody (G-9) (sc-365062) was used to standardize cytosolic protein loading on the sodium dodecyl sulfate-polyacrylamide gel electrophoresis. ROS1 (D4D6) rabbit mAbs from Cell Signaling Technology (catalog no: 3287) were used to recognize FIG-ROS1 and Phospho-ROS1 activity (Tyr2274) (catalog no: 3078). Anti-GOPC/FIG antibody (MyBioSource: MBS421395) was used to detect FIG expression. p-Met antibody (Tyr 1365) (sc-3408), p-Met (F-5) (sc-377548), p-ALK antibody (Tyr 1586) (sc-109905), Bim (H-191) (sc-11425), survivin (D-8) (sc-17779), Mcl-1 antibody (S-19) (sc-819), and p-Akt1/2/3 antibody (Ser 473)-R (sc-7985-R) were purchased from Santa Cruz Biotechnology, Inc. The secondary antibodies were horseradish peroxidase-conjugated goat anti-mouse immunoglobulin (Ig) G (ICN Biomedicals) and horseradish peroxidase-conjugated goat anti-rabbit IgG (ICN Biomedicals).

Caspase-3 colorimetric assays. Measurements of caspase-3 (Sigma) activity were performed using the commercially available assay kits. Concentration of pNA released from the substrate was calculated on the basis of absorbance values at 405 nm. The experiments were performed in triplicate.

Statistical analysis. All data were expressed as mean ± SEM values from the indicated number of experiments. Data were analyzed by one-way analysis of variance and Student's *t*-test. Variations were considered to be statistically significant at a *P* value of $^{*}P < 0.05$ or $^{**}P < 0.01$.

Results

Demographic and clinical characteristics of GB subjects. The mean age of the GB patients was 62 ± 10.81 years, with 12 men and 7 women in the experimental group; clinical treatment and outcome information from all patients is summarized in Table 1. GB patients without any prior procedures underwent MRI of the brain using standard sequences with and without gadolinium contrast. Samples from tumor regions were collected for slice culture analysis and IHC staining. Our IHC staining confirmed their astrocyte (GFAP) and protein expression. The proliferative activity was assessed by Ki-67 immunostaining in a subset of tumor tissue cultures ($n = 10$; Fig. 1A). As expected, GB stained positive for GFAP (astrocyte markers) and Ki-67 (proliferation markers; Fig. 1). Tissue samples from the tumor regions of 15 patients reveal distinct FIG-ROS1, p-ALK, and p-Met expression patterns (Fig. 1B). Statistical analysis showed that there were no significant differences in FIG-ROS1, p-ALK, and p-Met between the patients ($P \geq 0.1$). However, we saw little or no expression of FIG-ROS1, p-ALK, and p-Met in four GB patients. This may be due to a mutation or deletion of ALK and Met genes or a lack of fusion proteins.

Synergistic effects of crizotinib and temozolomide in FIG-ROS1 fusion-positive GB cells and tissue slices. Because U118 cells and FIG-ROS1-positive GB tissues express a significant level of phosphorylated ALK, Met, and ROS that are potently carcinogenic, we examined whether the combination of crizotinib and temozolomide might have an impact on the growth and survival of these cells. We performed MTT assay to determine the cell viability or death after 48 hours exposure of FIG-ROS1-positive cells and tissue slices with crizotinib alone or in combination with temozolomide. Cells and tissue slices treated with crizotinib or temozolomide each elicited 20.2% and 20.1% cell death, respectively, while the combination treatments with crizotinib and temozolomide resulted in a dramatic 80.1% cell death (Fig. 2A and C). Our results also demonstrated significantly increased ROS production and caspase-3 activity in the combinational treatments. This synergistic effect or similar potentiation of effect on cell death was observed in the U118 cell line by flow cytometry using the Annexin V-FITC Apoptosis Detection Kit (Fig. 2B). We were also able to correlate molecular changes due to apoptosis with internucleosomal DNA fragmentation in FIG-ROS1-positive tissues. Unlike untreated cells, substantial DNA laddering was found in cells treated with the combination of crizotinib and temozolomide (Fig. 2D).

Combinatorial blockade of p-ALK, p-Met, and FIG augmented apoptosis, which mechanistically involves activation of Bim and inhibition of oncogenic markers. Importantly, we showed the utility of this in vitro and ex vivo model in potentially predicting tumor sensitivity to drugs in

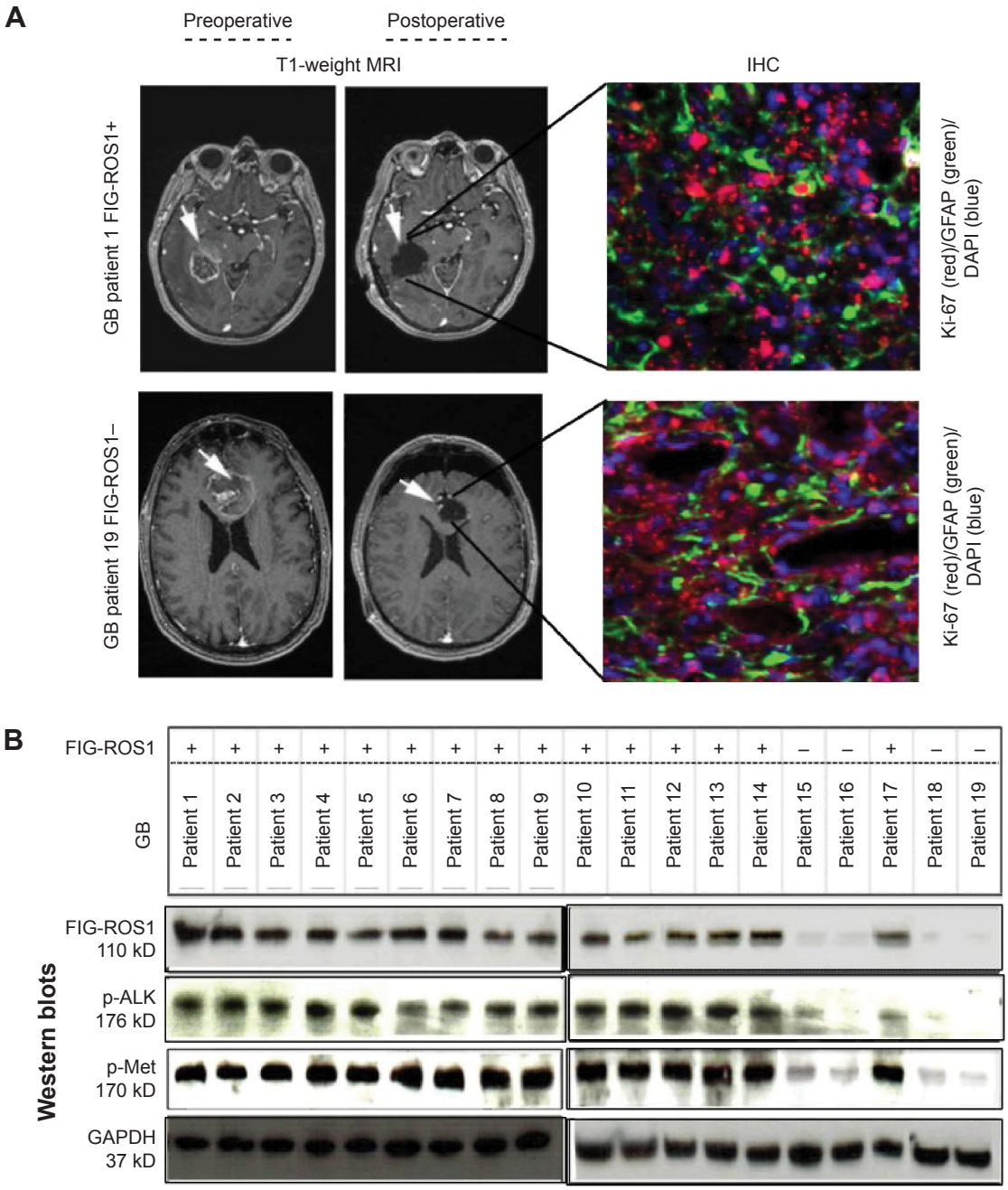

Figure 1. Analysis of pre- and postoperative T1-weighted MRI with gadolinium (**A**), IHC (**A**), and Western blots (**B**) of collected FIG-ROS1 ± GB tumor samples. Tissue samples from the tumor regions of 15 patients reveal distinct FIG-ROS1, p-ALK, and p-Met expression patterns. GB tumor (white arrows; **A**) stained for astrocytic (GFAP) and proliferation (Ki-67) markers (Ki-67-red; GFAP-green; DAPI-blue). (**B**) Representative Western blots for FIG-R0S1, p-ALK, p-Met, and GAPDH are shown in the surgically collected GB tumor samples.

a patient-specific manner. Given that crizotinib and temozolomide induced apoptosis in FIG-ROS1-positive GB cells and tissue slices, we examined the effects of crizotinib alone or in combination with temozolomide on the expression of FIG, p-ROS1, p-ALK, and p-Met. Our results demonstrated that untreated FIG-ROS1-positive GB tumors showed constant levels of FIG, p-ROS1, p-ALK, and p-Met that decreased dramatically after in vitro and ex vivo treatments with crizotinib and combination therapy with crizotinib plus temozolamide.

Furthermore, crizotinib downregulated the expression of survivin, a member of the inhibitor of apoptosis protein (IAP) family in FIG-ROS1-positive GB; this effect was greatly enhanced by the addition of temozolomide (Fig. 3A). Further analysis indicated that a well-established survival protein, Mcl-1, was significantly reduced by combination treatments of crizotinib and temozolomide (Fig. 3C–F). Crizotinib upregulated the expression of BIM, a pro-apoptotic member of the Bcl-2 family of proteins, in FIG-ROS1-positive cell lines. This effect was also greatly enhanced in cells under

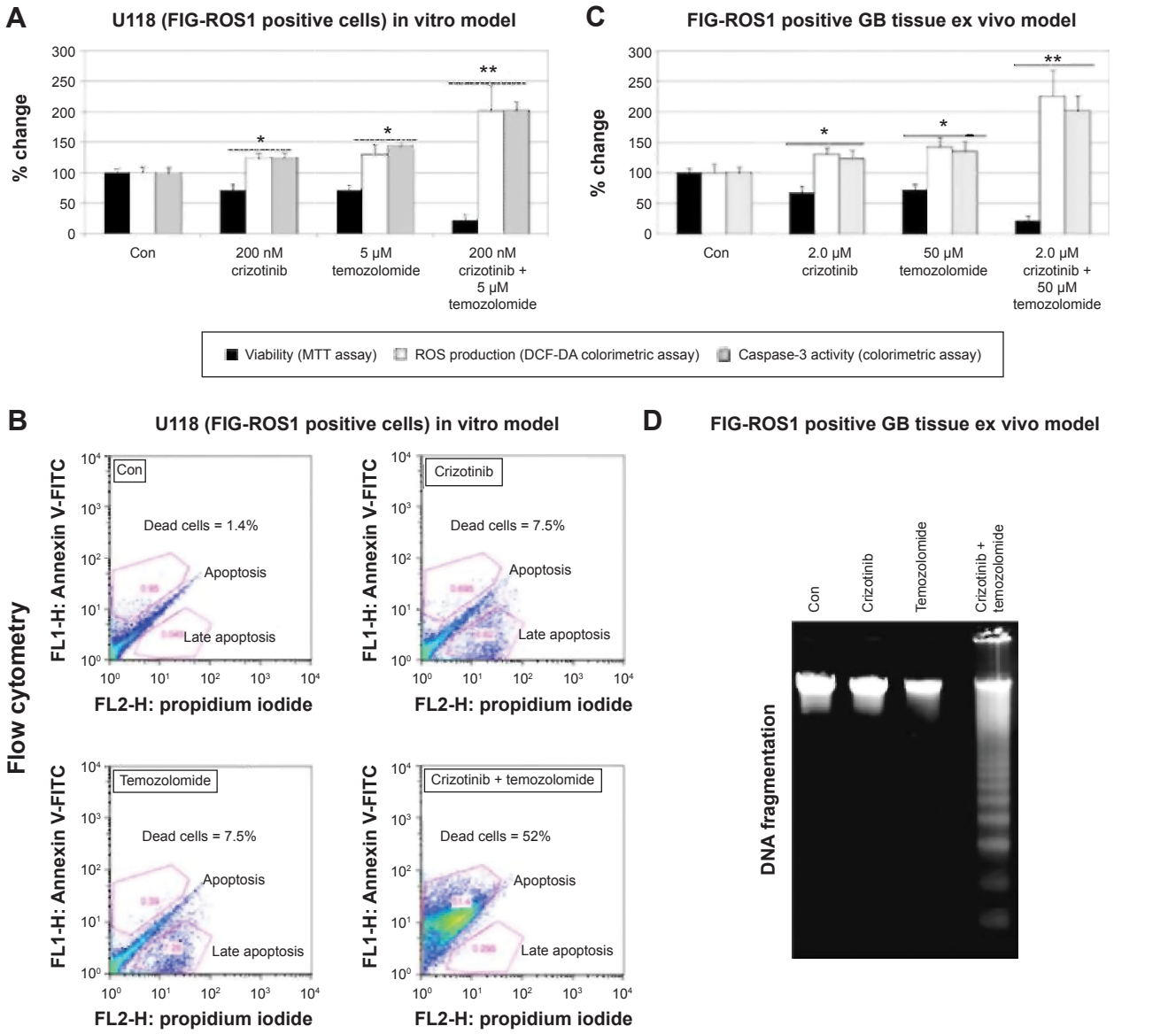

Figure 2. Synergistic effects of crizotinib and temozolomide in FIG-ROS1 fusion-positive GB cells. Quantification analyses of viabilities (MTT assay), ROS production (DCF-DA fluorometric assay), and caspase-3 activity (colorimetric assay) in in vitro (**A**) and ex vivo (**C**) FIG-ROS1-positive GB. Cell death was also confirmed by flow cytometry (**B**) in in vitro (U118) and DNA fragmentation (**D**) in ex vivo (slice culture) models. Treatments: Con, crizotinib, temozolomide, and crizotinib + temozolomide (*$P < 0.05$ and **$P < 0.01$).

combination treatments, which correlated with a more complete blockade in FIG, p-ROS1, p-ALK, and p-Met. Thus, these data suggest that the combination of crizotinib and temozolomide better inhibits the phosphorylation of ROS1, ALK, and Met (resulting in induction of apoptosis) than crizotinib alone in FIG-ROS1-positive GB cells and tissue slices.

Partial effects of crizotinib and temozolomide in FIG-ROS1-negative GB cells and tissue slices. We next examined the combinational effects of crizotinib and temozolomide on FIG-ROS1-negative cells (U87MG) and glioma tissues (GBpt15, GBpt16, GBpt18, and GBpt19). Cell viability and caspase-3 assay were determined by MTT and caspase-3 colorimetric assay. The concentration of drugs required to obtain a 25% inhibition (IC25) of proliferation in vitro was used to test the effectiveness of the crizotinib and temozolomide combination in the cell lines. A beneficial effect of the simultaneous use of both drugs was not observed to the same degree as compared to FIG-ROS1-positive cells. The exposure to the two drugs induced an effect that was less potent than that would be expected from the sum of the effects that each drug would produce on its own. One drug, therefore, possibly counteracted some of the effects of the other. Thus, our data suggested that crizotinib inhibits the phosphorylation of ROS1, ALK, and Met, resulting in sensitizing induction of apoptosis, in FIG-ROS1-positive cells, but such effects were not observed in FIG-ROS1-negative cells, including those with low levels of ALK and Met (Fig. 4A and B).

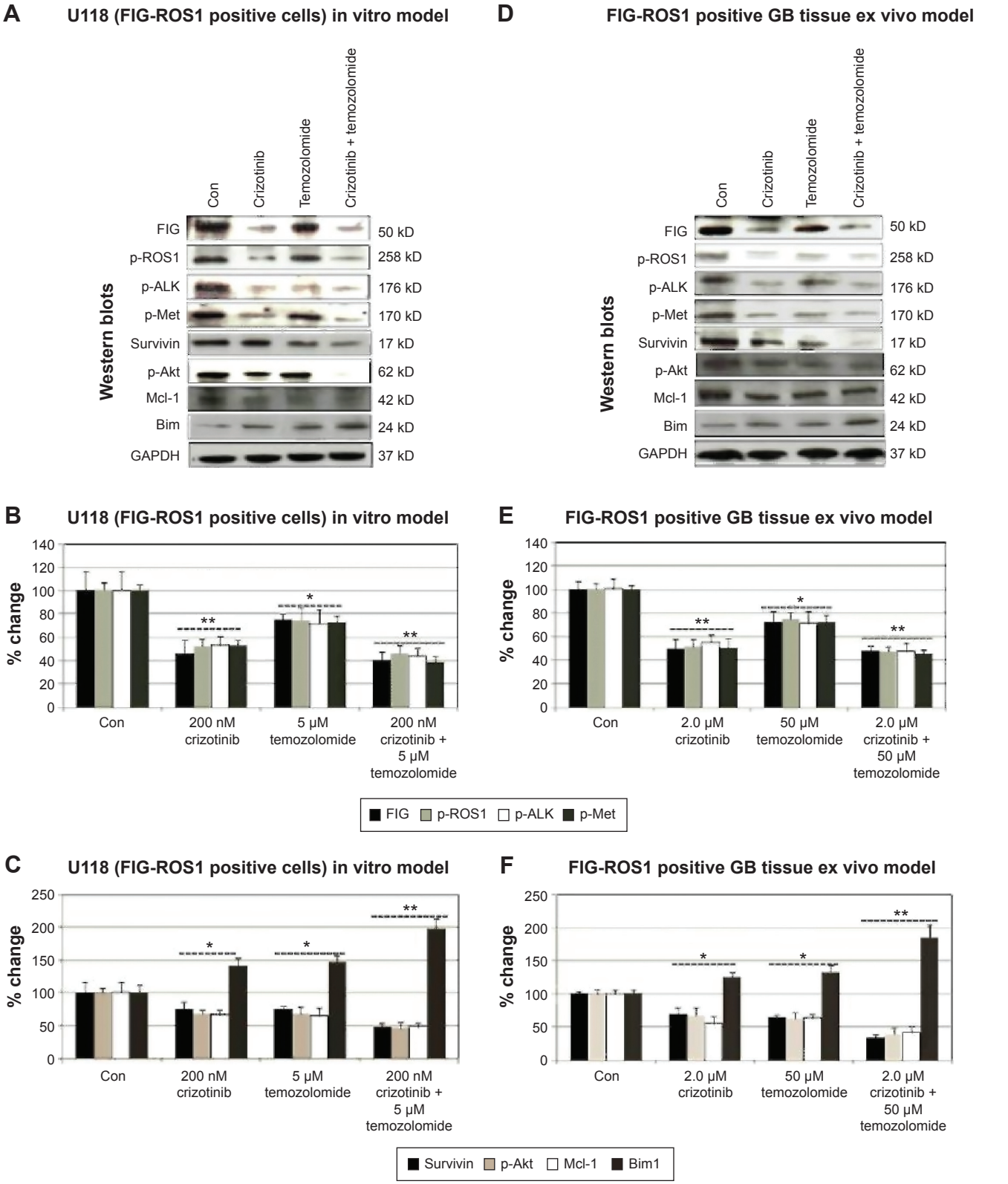

Figure 3. Combinatorial blockade of FIG, ROS1, p-ALK, and p-Met by crizotinib and temozolomide suppresses GB anti-apoptotic gene and activates pro-apoptotic gene. Representative Western blots for FIG, ROS1, p-ALK, p-Met, survivin, p-Akt, Mcl-1, and Bim are shown in in vitro (**A**) and ex vivo (**D**) models. Quantification of blot signals relative to GAPDH confirmed significant downregulation of FIG, ROS1, p-ALK, p-Met, survivin, p-Akt, and Mcl-1 concurrent with a significant activation of Bim in in vitro (U118) (**B**, **C**) and in ex vivo (slice culture) (**E**, **F**) models. Data taken from FIG-ROS1-positive U118 (in vitro) and 15 GB (ex vivo) samples. Treatments: Con, crizotinib, temozolomide, and crizotinib + temozolomide (*$P < 0.05$ and **$P < 0.01$).

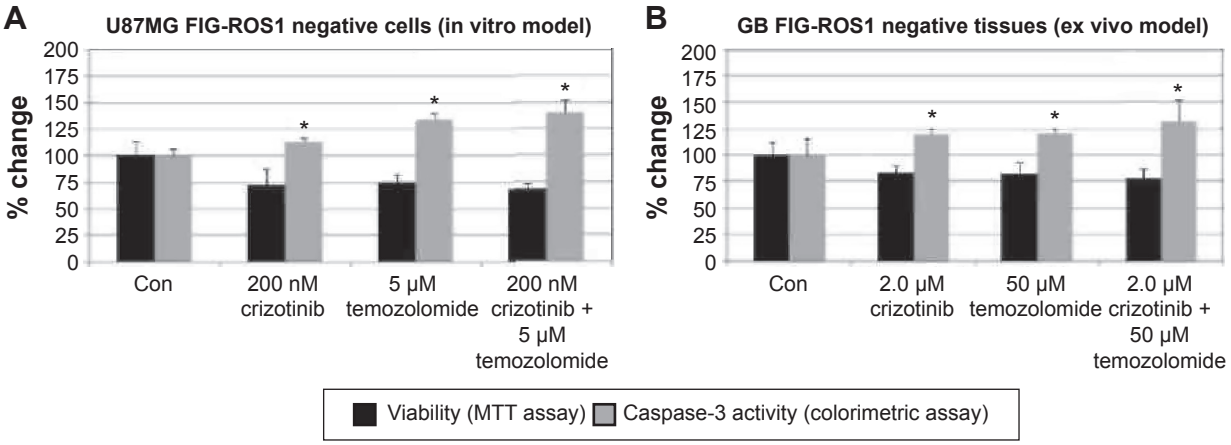

Figure 4. Partial effects of crizotinib and temozolomide on FIG-ROS1-negative GB cells and tissue slices. Quantification analysis of viabilities (MTT assay) and caspase-3 activity (colorimetric assay) in in vitro (U87MG: **A**) and ex vivo (slice cultures: **B**) FIG-ROS1-negative GB. Data taken from FIG-ROS1-negative U87MG (in vitro) and four GB samples. Treatments: Con, crizotinib, temozolomide, and crizotinib + temozolomide (*$P < 0.05$).

Discussion

Tyrosine kinase inhibitors (TKIs) targeted to ALK/Met are undergoing clinical trials in GB patients, but the precise mechanism of the antitumor activity or drug resistance of these drugs remains unclear.[7] Several TKIs are currently undergoing clinical trials in GBs. Because it is the most common primary intracranial malignancy and due to the relatively poor clinical outcomes characterized by this disease, it is important to identify the patient subgroups that might actually benefit from treatment with such drugs in order to optimize their efficacy by providing more targeted therapy. To help accomplish this goal, using ex vivo organotypic short-term culture of tumor will allow us to determine which pathway activation and pharmacologic inhibition can be rapidly studied with respect to the native heterogeneity of a patient's tumor. The drug crizotinib (Pfizer, Inc.; which blocks ALK and c-Met) that has been the only TKI in clinical studies until 2010 is now on the market after showing robust response rates in early trials.[9] Translation of crizotinib for use in locally advanced GB patients will largely depend on a better understanding of the effects elicited by this novel class of dual ALK/c-Met inhibitors in combination with temozolomide (chemotherapeutic agent used in the current standard of care). Thus, we examined the antitumor action of crizotinib alone and in combination with temozolomide in GB cells in in vitro and ex vivo models that are positive or negative for FIG-ROS1.

Given that crizotinib showed inhibitory effects of the phosphorylation of ROS1, ALK, and Met in FIG-ROS1-positive GB cells in in vitro and ex vivo models, we further investigated the effect of crizotinib alone and in combination with temozolomide in these cells. We found that crizotinib selectively augments pro-apoptotic effects of temozolomide in GB tumors harboring FIG-ROS1 fusion. In contrast, dual therapy with crizotinib and temozolomide may exert inferior efficacy in tumors that lack ALK/Met activation or FIG-ROS1 gene. These data clearly suggest tumor utilization of ALK/Met signaling as a prerequisite for the observed temozolomide-sensitizing effect of crizotinib. Our data unequivocally indicate beneficial effects of crizotinib and temozolomide in FIG-ROS1 fusion-harboring GB. Therefore, this study constitutes a critical step toward clinical translation of this favorable combination to use in the treatment of GB.

Our data also demonstrated that crizotinib alone or in combination with temozolomide suppresses the AKT signaling pathway through the downregulation of survivin expression (a member of the IAP family that protects cells against apoptosis by either directly or indirectly inhibiting the activation of effector caspases). Interestingly, the combination of crizotinib and temozolomide also downregulated Mcl-1 expression and displaced the activator BH3-only protein, Bim, from the Mcl-1:Bim complex. This triggered mitochondrial dysfunction, caspase activation, and ultimately apoptosis. Feeding into this pathway is the direct activation of caspase-3, which alone does not appear to be sufficient to trigger significant levels of cell death. However, these activated caspases may also contribute to the observed downregulation of Mcl-1 expression following crizotinib and temozolomide treatment. This is because they have been shown to mediate cleavage of Mcl-1 and loss of Mcl-1 expression, thereby further freeing the Bim protein from the Mcl-1:Bim complex. Furthermore, we also found that coinhibition of ALK/Met signaling by crizotinib and temozolomide not only resulted in the induction of apoptosis but also was accompanied by the inhibition of AKT and survivin in GB cells. This was shown in FIG-ROS1-positive GB cells but not in FIG-ROS1-negative GB cells. These results thus suggest that ALK/Met signaling is essential for the survival of FIG-ROS1-positive cells but not for that of

FIG-ROS1-negative cells (Fig. 4). Our present study, therefore, suggests that crizotinib may have little clinical efficacy in patients with FIG-ROS1-negative GB but significant efficacy in FIG-ROS1-positive GB. Evidence has recently emerged from multiple laboratories, which shows that crizotinib monotherapy in different cancers exerted a transient tumor growth delay in ROS1 (CD74-ROS1), ALK, and Met mutation cells or led to the development of crizotinib resistance, the advent of which was prolonged by the addition of temozolomide.[21] Further studies are needed to uncover the mechanisms governing inherent and acquired resistance to crizotinib or ROS1 (CD74-ROS1), ALK, and Met mutation.

In conclusion, our analysis of the combinational effects of crizotinib and temozolomide on the growth of GB cells ex vivo revealed that this combination had a pronounced antitumor effect on FIG-ROS1-positive tissues but not so much on FIG-ROS1-negative tissues. These ex vivo data are consistent with our results obtained in vitro. The finding that crizotinib effectively sensitizes a tumor to temozolomide in a FIG-ROS1 experimental model suggests that further evaluation of this combination may be a promising strategy for GB therapy. For combination studies, a key issue is likely to be concerning over the potential for increased normal tissues surrounding tumor toxicity and identifying the combinations and schedules that have the greatest potential for GB selective effects. This is a priority area of research that needs further investigation on orthotopic xenograft models or patient-derived xenograft models with mutation or deletion of ALK and Met gene or lack of fusion proteins. Following the progress of these approaches will be of great interest, and the use of the emerging results will better guide future clinical development.

Acknowledgments

This study used the services of the MUSC Flow Cytometry Facility, which is supported by NIH-NIGMS P30 GM103342 to the South Carolina COBRE for Developmentally Based Cardiovascular Diseases. Alyssa Pierce assisted with revision of the final manuscript.

Author Contributions

Conceived and designed the experiments: AD and PG. Analyzed the data: RRC, AD, PG, and YND. Wrote the first draft of the manuscript: AD, PG. Contributed to the writing of the manuscript: AD, WV, PG, SJP, SML, MD, DC, AKV, NLB, RRC, MLTH, and YND (all authors). Agree with manuscript results and conclusions: All authors. Jointly developed the structure and arguments for the paper: All authors. Made critical revisions and approved final version: AD and PG. All authors reviewed and approved of the final manuscript.

REFERENCES

1. Burton EC. Malignant gliomas. *Curr Treat Options Oncol*. 2000;1(5):459–468.
2. Alentorn A, Duran-Peña A, Pingle SC, Piccioni DE, Idbaih A, Kesari S. Molecular profiling of gliomas: potential therapeutic implications. *Expert Rev Anticancer Ther*. 2015;15(8):955–962.
3. Kamiya-Matsuoka C, Gilbert MR. Treating recurrent glioblastoma: an update. *CNS Oncol*. 2015;4(2):91–104.
4. *Central Brain Tumor Registry of the United States*. 2012. Available at: http://www.cbtrus.org/
5. Gao CF, Vande Woude GF. HGF/SF-Met signaling in tumor progression. *Cell Res*. 2005;15:49–51.
6. Pulford K, Morris SW, Turturro F. Anaplastic lymphoma kinase proteins in growth control and cancer. *J Cell Physiol*. 2004;199:330–358.
7. Wallace GC IV, Dixon-Mah YN, Vandergrift WA III, et al. Targeting oncogenic ALK and MET: a promising therapeutic strategy for glioblastoma. *Metab Brain Dis*. 2013;28(3):355–366.
8. Zou HY, Li Q, Lee JH, et al. An orally available small-molecule inhibitor of c-Met, PF-2341066, exhibits cytoreductive antitumor efficacy through antiproliferative and antiangiogenic mechanisms. *Cancer Res*. 2007;67:4408–4417.
9. Kwak EL, Camidge DR, Clark J, et al. Clinical activity observed in a phase I dose escalation trial of an oral c-met and alk inhibitor, PF-02341066. *J Clin Oncol*. 2009;27(suppl: Abstr 3509):15s.
10. Bang Y, Kwak EL, Shaw AT, et al. Clinical activity of the oral ALK inhibitor PF-02341066 in ALK-positive patients with non-small cell lung cancer (NSCLC). *J Clin Oncol*. 2010;28(suppl: Abstr 3):18s.
11. Park J, Yoshida K, Kondo C, et al. Crizotinib induced esophageal ulceration: a novel adverse event of crizotinib. *Lung Cancer*. 2013;81(3):495–496.
12. Takeda M, Okamoto I, Nakagawa K. Clinical impact of continued crizotinib administration after isolated central nervous system progression in patients with lung cancer positive for ALK rearrangement. *J Thorac Oncol*. 2013;8(5):654–657.
13. Pennell NA. Treating anaplastic lymphoma kinase-positive lung cancer in the weeks after the US Food and Drug Administration approval of crizotinib. *J Oncol Pract*. 2012;8(3 suppl):34s–37s.
14. Charest A, Kheifets V, Park J, et al. Oncogenic targeting of an activated tyrosine kinase to the Golgi apparatus in a glioblastoma. *Proc Natl Acad Sci U S A*. 2003;100:916–921.
15. Birchmeier C, O'Neill K, Riggs M, Wigler M. Characterization of ROS1 cDNA from a human glioblastoma cell line. *Proc Natl Acad Sci U S A*. 1990;87(12):4799–4803.
16. Birchmeier C, Sharma S, Wigler M. Expression and rearrangement of the ROS1 gene in human glioblastoma cells. *Proc Natl Acad Sci U S A*. 1987;84(24):9270–9274.
17. Charest A, Lane K, McMahon K, et al. Fusion of FIG to the receptor tyrosine kinase ROS in a glioblastoma with an interstitial del(6)(q21q21). *Genes Chromosomes Cancer*. 2003;37(1):58–71.
18. Bos M, Gardizi M, Schildhaus HU, et al. Complete metabolic response in a patient with repeatedly relapsed non-small cell lung cancer harboring ROS1 gene rearrangement after treatment with crizotinib. *Lung Cancer*. 2013;81(1):142–143.
19. Yanagisawa S, Inoue A, Koarai A, Ono M, Tamai T, Ichinose M. Successful crizotinib retreatment after crizotinib-induced interstitial lung disease. *J Thorac Oncol*. 2013;8(8):e73–e74.
20. Gautschi O, Schefer H, Riklin C, Strobel K, Diebold J. Experience in integrating ALK testing and crizotinib into the routine treatment of patients with non-small cell lung cancer. *Onkologie*. 2013;36(6):342–347.
21. Awad MM, Katayama R, McTigue M, et al. Acquired resistance to crizotinib from a mutation in CD74-ROS1. *N Engl J Med*. 2013;368(25):2395–2401.
22. Xia P, Gou WF, Zhao S, Zheng HC. Crizotinib may be used in Lewis lung carcinoma: a novel use for crizotinib. *Oncol Rep*. 2013;30(1):139–148.
23. Merz F, Gaunitz F, Dehghani F, et al. Organotypic slice cultures of human glioblastoma reveal different susceptibilities to treatments. *Neuro Oncol*. 2013;15(6):670–681.
24. Das A, Miller R, Lee P, et al. A novel component from citrus, ginger, and mushroom family exhibits antitumor activity on human meningioma cells through suppressing the Wnt/β-catenin signaling pathway. *Tumor Biol*. 2015. PMID: 25864108.
25. Wallace GC IV, Haar CP, Vandergrift WA III, et al. Multi-targeted DATS prevents tumor progression and promotes apoptosis in ectopic glioblastoma xenografts in SCID mice via HDAC inhibition. *J Neurooncol*. 2013;114(1):43–50.
26. Das A, Banik NL, Ray SK. Flavonoids activated caspases for apoptosis in human glioblastoma T98G and U87MG cells but not in human normal astrocytes. *Cancer*. 2010;116(1):164–176.
27. Powers C, Aigner A, Stoica GE, McDonnell K, Wellstein A. Pleiotrophin signaling through anaplastic lymphoma kinase is rate-limiting for glioblastoma growth. *J Biol Chem*. 2002;277(16):14153–14158.